View metadata, citation and similar papers at core.ac.uk
brought to you by CORE

東北大学機関リポジトリ
TOUR
Tohoku University Repository

Quantum chemical study on the oxidation process of a hydrogen terminated Si surface

著者	宮本　明
journal or publication title	Journal of Chemical Physics
volume	109
number	4
page range	1495-1504
year	1998
URL	http://hdl.handle.net/10097/46787

doi: 10.1063/1.476700

Quantum chemical study on the oxidation process of a hydrogen terminated Si surface

Kazuo Teraishi, Hiromitsu Takaba, Aruba Yamada, Akira Endou, Isao Gunji, Abhijit Chatterjee, Momoji Kubo, and Akira Miyamoto[a)]
Department of Materials Chemistry, Graduate School of Engineering, Tohoku University, Aoba, Aramaki, Aoba-ku, Sendai, 980-8579, Japan

Kazutaka Nakamura and Masahiro Kitajima
National Research Institute for Metals, 1-2-1, Sengen, Tsukuba, Ibaragi, 305, Japan

(Received 3 March 1998; accepted 17 April 1998)

The initial oxidation process of a hydrogen terminated Si surface was investigated by molecular orbital calculations using the cluster models representing H–Si(100)-2×1 and H–Si(111)-1×1. *Ab initio* calculations using small cluster models revealed that as a Si atom is coordinated by more oxygen atoms, it increases the affinity toward another oxygen. Furthermore, the insertion of up to five oxygen atoms into Si–Si bonds of large models were traced by the semiempirical AM1 method, whose reliability was proven by comparison with *ab initio* results. The structural relaxation was suggested to be as important as the electronic effect on the stability of oxides, and on the H–Si(111)-1×1 surface oxidation was predicted to proceed to the second layer before its completion on the first layer to avoid a large strain which otherwise would be caused. It was also revealed that on the H-Si(100)-2×1 surface, the growth of the oxide island and the nucleation of oxide at a distant site have almost the same probabilities. In contrast, the lateral growth of the oxide island is preferred to the formation of an isolated oxide nuclei on the H-Si(111)-1×1 surface. These differences derive from the different Si–Si bond topology on each surface. © *1998 American Institute of Physics.* [S0021-9606(98)30528-0]

I. INTRODUCTION

In the ultralarge scale integrated circuit (ULSI) currently under development, such as 1 Gbit dynamic random access memory (DRAM), the thickness of the oxide film used as gate dielectrics in metal-oxide-semiconductor field-effect transistors (MOSFETs) corresponds to nearly or even less than ten molecular layers. With the reduction of oxide film thickness, the atomic level structure at the SiO_2/Si interface becomes crucial in the gate dielectric reliability such as leakage current or dielectric breakdown. Atomic scale control of the oxidation process is, therefore, an urgent task in the semiconductor industry. As the thickness of the gate oxide is comparable to the native oxide formed on the clean Si surface, use of the passivated surfaces, on which active dangling bonds are saturated with hydrogen, has been explored. The technique is already established to realize the atomically flat hydrogen terminated Si(100)-2×1[1] and Si(111)-1×1[2] surfaces, and their oxidation process has also been studied in detail by various experimental analyses, e.g., x-ray photoelectron spectroscopy (XPS),[3–8] IR,[6–8] atomic force microscope (AFM),[7,9] scanning tunneling microscopy/scanning tunneling spectroscopy (STM/STS),[10] and high-resolution electron energy-loss spectroscopy (HREELS).[11,12]

Efforts have been made to clarify the effect of surface hydrogen on the oxidation process in various conditions.[5,7,8,13] Nakamura *et al.*[13] investigated the sticking probability of molecular oxygen on the Si(111) surface at room temperature as a function of preadsorbed hydrogen. They found that the sticking probability decreases as the hydrogen exposure is increased. Kurokawa *et al.*[5] reported that the oxidation by molecular oxygen decreases to become negligible as the amount of hydrogen exposure is increased on the Si(111) surface at 50 °C, while that by ozone is also reduced but not completely. Miura *et al.*,[8] on the other hand, monitored the surface Si–H stretching band on hydrogen terminated Si(100) and Si(111) surfaces and the thickness of native oxide formed on them in room air, and found that when the surface hydrogen coverage diminishes, native oxide thickness starts to increase sharply. Therefore, oxidation on the hydrogen passivated surface is undoubtedly slow, and one may infer that oxygen would diffuse on the surface and find energetically favorable sites before the reaction takes place. The importance of a hydrogen terminated surface in practical applications should also be emphasized because the preoxidation of the hydrogen terminated Si(100) surface at 300 °C followed by thermal oxidation at 900 °C reportedly yields a smoother surface than the oxide formed without preoxidation.[7]

The oxidation process of particularly important surfaces, namely, H–Si(100)-2×1 and H–Si(111)-1×1, has been studied rigorously and some differences have been pointed out. Ohishi *et al.*[3] investigated the changes in Si 2p photoelectron spectra during the oxidation of H–Si(111)-1×1 and discovered that the densities of Si^{1+}, which is bonded to one oxygen and three silicon atoms, and Si^{3+}, which is bonded to three oxygen and one silicon atoms, oscillate in opposite

[a)]Author to whom correspondence should be addressed.

 © 1998 American Institute of Physics

Downloaded 22 Feb 2010 to 130.34.135.21. Redistribution subject to AIP license or copyright; see http://jcp.aip.org/jcp/copyright.jsp

phase. The oxidation was thus suggested to proceed layer-by-layer, which was also supported by the periodic change in surface microroughness observed by AFM.[9] On the contrary, no evidence for the layer-by-layer growth was discovered in the case of H–Si(100)-2×1 oxidation from XPS measurements.[4] Ikeda *et al.*[11,12] reported that the energy loss peaks of the Si–O–Si asymmetric stretching mode on hydrogen terminated Si(100)-1×1(dihydride) and -2×1(monohydride) surfaces are constant at low oxygen coverage, which indicates that the first oxidation step on these surfaces is a simple adsorption without the structural relaxation. In contrast, the energy loss increased monotonously as a function of oxygen coverage on H–Si(111)-1×1, which is similar to the behavior on the clean Si(100) surface rather than on the H-terminated one. Hattori *et al.*[6] performed the simulations of oxidation process based on the bonding probabilities of Si atoms to oxygen which were determined to reproduce the experimental data, and analyzed the distribution of oxygen. According to their results, once the isolated bridging oxygen atoms are produced, the oxidation proceeds in lateral direction around these oxygen atoms on H–Si(111)-1×1, while in the case of H–Si(100)-2×1, oxygen atoms are distributed more uniformly, i.e., the sizes of oxide clusters on the Si(100) surface are smaller than those on the Si(111) surface. The origin of these differences is, however, not fully understood.

Furthermore, the initial oxidation sites on a hydrogen terminated Si(100)-2×1 reconstructed surface are still controversial. From the surviving σ-antibonding state corresponding to a Si dimer detected by STS measurements and the absence of the symmetric stretching and bending modes of Si–O–Si in HREELS during the initial oxidation of the H–Si(100)-2×1 surface, Ohmori *et al.*[10] concluded that the adsorption site of oxygen is not the Si dimer bonds but the backbonds of Si dimer atoms. Hattori *et al.*,[6] on the other hand, discovered the Si–H stretching associated with Si coordinated by three oxygen atoms in IR adsorption spectra at the early oxidation stage of H–Si(100)-2×1, which indicates that the dimer bonds, as well as backbonds, are bridged by oxygen.

The best way to sort out the aforementioned ambiguities is to observe the process of oxygen insertion into Si bonds one by one, which is, however, not accessible experimentally. Theoretical simulation has become a powerful tool to analyze the target at atomic resolution, and has been applied to study the chemistry of the Si surface. The initial oxidation, i.e., adsorption, dissociation, and migration of oxygen, on clean Si(100)-2×1[14–18] and Si(111)-7×7[18–20] surfaces was exhaustively studied by extended Hückel,[14,19] semiempirical modified neglect of differential overlap (MNDO),[18] and first principle Hartree–Fock (HF)[15,16] and density functional theory (DFT),[17,20] using periodic slab[15,17,19,20] or cluster[14,16,18] models. The hydrogen terminated surface, in particular the Si(100) surface which appears with 1×1, 2×1, or 3×1 symmetry depending on the environment, was also subjected to the computational analyses, and the structure along with the adsorption/desorption mechanism of hydrogen on the surface were investigated by semiempirical

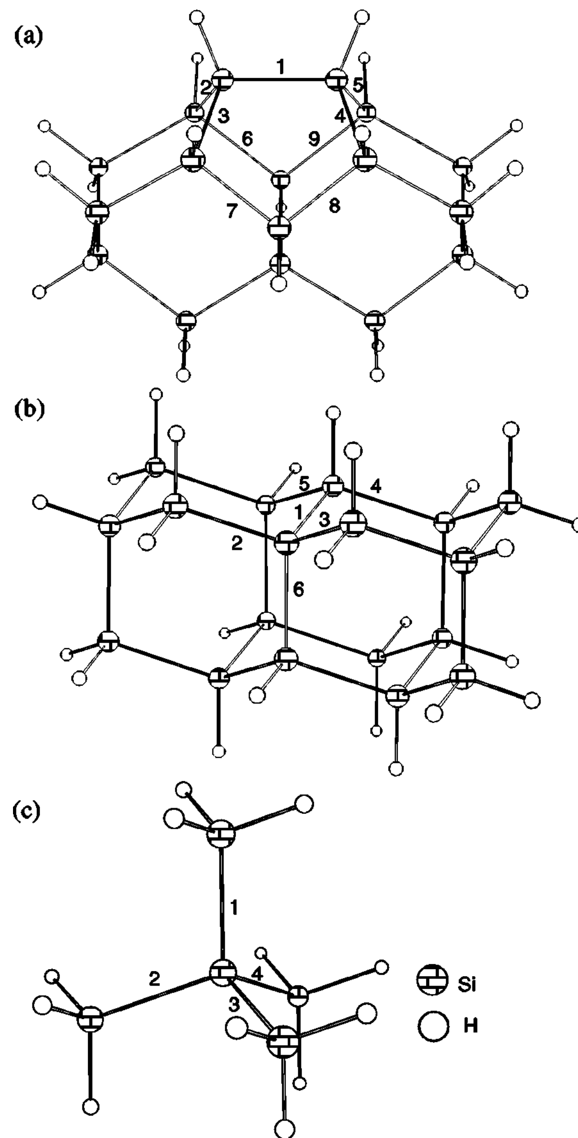

FIG. 1. Small models for (a) H–Si(100)-2×1 and (b) H–Si(111)-1×1 surfaces and (c) $Si(SiH_3)_4$ molecule. The numbers indicate the positions for oxygen insertions.

MINDO[21,22] and PM3,[23] and *ab initio* HF and post-HF methods[24] and DFT.[25]

In spite of its importance, however, very few theoretical studies on the oxidation of hydrogen terminated surface have been reported.[26] Furthermore, although a few layers of oxide are formed even at the initial oxidation, most of the theoretical works so far dealt only with the surface reaction. The purpose of this paper is, therefore, to clarify the oxidation process of hydrogen terminated Si(100)-2×1 and Si(100)-1×1 surfaces at atomic resolution, achievement of which was sought by tracing the insertion of each oxygen atom into Si–Si bonds by means of molecular orbital calculations in combination with cluster models. The change in the electronic structure upon the formation of Si–O bonds was investigated at first by *ab initio* methods using small cluster models. Also from the comparison with *ab initio* results, the semiempirical AM1 method was proven to be reliable in the prediction of the stability order of different oxygen configurations. In order to appropriately take into account the geom-

Downloaded 22 Feb 2010 to 130.34.135.21. Redistribution subject to AIP license or copyright; see http://jcp.aip.org/jcp/copyright.jsp

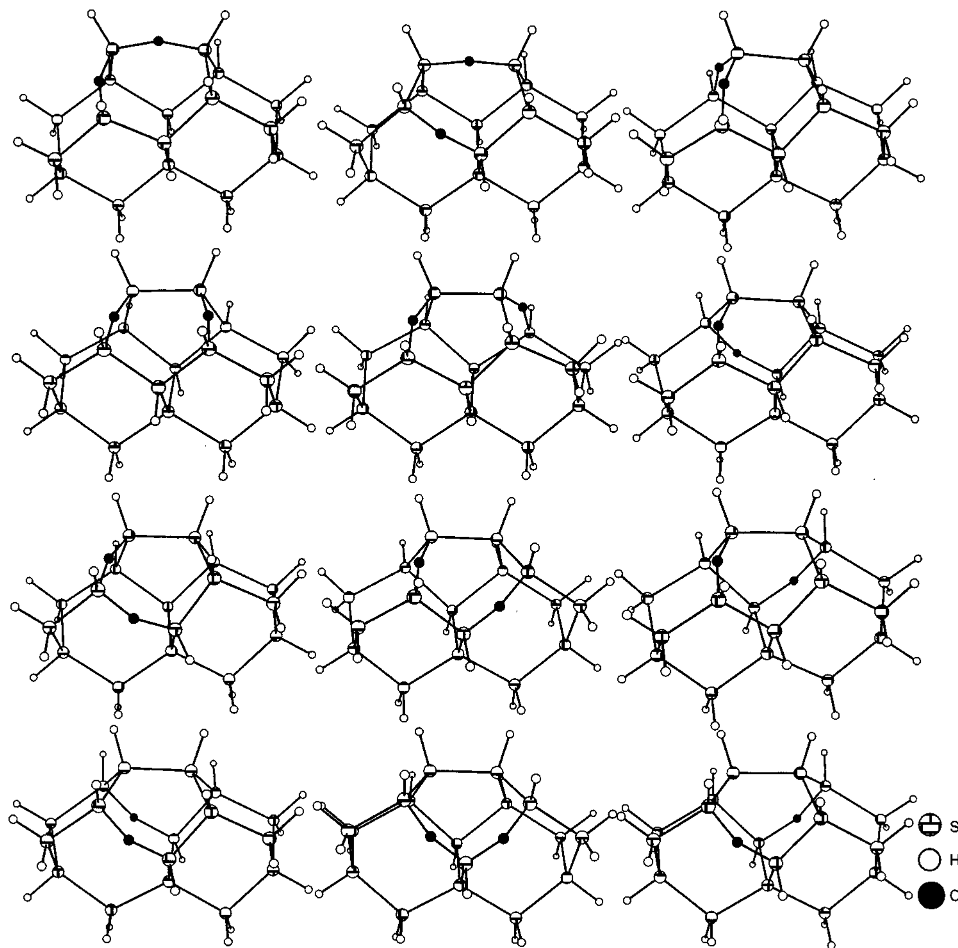

FIG. 2. Twelve oxygen configurations when two oxygen atoms are inserted into the H–Si(100)-2×1 small model.

etry relaxation energy, the large cluster models of H–Si(100)-2×1 and H–Si(111)-1×1 were constructed, and the oxidation process of each surface was calculated and compared using the AM1 method.

II. COMPUTATIONAL DETAILS

In order to investigate the chemistry of Si–O bonds, *ab initio* molecular orbital calculations were performed using the relatively small cluster models expressing H–Si(100)-2×1 and H–Si(111)-1×1 surfaces [Figs. 1(a) and 1(b), respectively]. In these models, dangling bonds on the boundary which were introduced at the extraction of models were saturated with hydrogen atoms. These models were selected with care so as to avoid the collision between terminal hydrogen atoms. All possible structures possessing from 1 to 5 oxygen atoms inserted into 9 or 6 Si–Si bonds marked with numbers in Figs. 1(a) and 1(b) were constructed, and the bonding energies were calculated. Oxidation of Si–H bonds was not considered here because the oxidation of an Si–Si bond is observed experimentally at an early oxidation stage of the hydrogen terminated surface,[6,8,11,12] and also from our preliminary calculations, oxygen insertion was found to take place more favorably into Si–Si bonds than into Si–H bonds. Also as a reference, insertions of 1–4 oxygen atoms into four Si–Si bonds of pentasilane molecule [Fig. 1(c)] were examined.

As for H–S(100)-2×1, the structures obtained when one oxygen atom is inserted at one of the positions marked from 2 to 5 are identical due to the symmetry. Likewise, the structures with oxygen at one of the positions marked from 6 to 9 are all equivalent. Therefore, there are three configurations with one inserted oxygen. When two oxygen atoms are inserted, there are 12 unequivalent configurations as shown in Fig. 2. Corresponding to the oxidation stages with 3, 4, and 5 oxygen atoms, there are 24, 36, and 36 configurations, respectively. All the configurations with 1 or 2 oxygen atoms were calculated by means of an *ab initio* molecular orbital method. Also for the same set of models, semiempirical AM1 calculations were carried out and the results were compared with those obtained by *ab initio* calculations. As discussed later, the stability order of oxygen configurations computed by AM1 agreed well with that obtained by *ab initio* calculations. Therefore, for the models with 3–5 inserted oxygen atoms, the energies of all the configurations were first calculated by AM1, out of which the five lowest-energy configurations with respective number of oxygen atoms were chosen to be calculated by *ab initio* method.

On the actual H–Si(111)-1×1 complete surface, all Si–Si bonds in the top layer are identical. Thus the position marked number 1 was always associated with oxygen, except for the case where only one oxygen was inserted into the second layer (position 6), and all the unequivalent oxygen configurations were constructed. Accordingly, corresponding

Downloaded 22 Feb 2010 to 130.34.135.21. Redistribution subject to AIP license or copyright; see http://jcp.aip.org/jcp/copyright.jsp

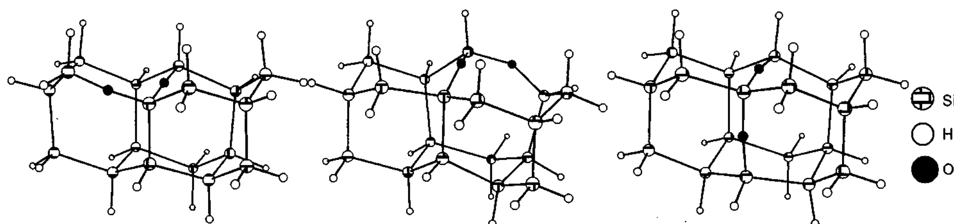

FIG. 3. Three oxygen configurations when two oxygen atoms are inserted into the H–Si(111)-1×1 small model.

to the number of oxygen atoms ranging from 1 to 5, the number of configurations are 2, 3, 6, 6, and 3, respectively. Three configurations with two oxygen atoms are shown in Fig. 3. All of these configurations were calculated by *ab initio* molecular orbital method.

Oxygen bonding energies were calculated as follows: $\Delta E = E(\text{Si–O}_{n-1}) + 1/2E(\text{O}_2) - E(\text{Si–O}_n)$. Here, $E(\text{Si–O}_{n-1})$ and $E(\text{Si–O}_n)$ are the total energies of the cluster models with $n-1$ and n inserted oxygen atoms, respectively, and $E(\text{O}_2)$ is the energy of oxygen molecule.

Small models described above are adequate to investigate the local nature of Si–O bonds, but would cause the overestimation of structural relaxation effect because no constraints are imposed on the deformation of clusters. The relative stability of oxygen configurations during the oxidation process should therefore be examined using more realistic models. The large cluster models shown in Figs. 4(a) and 4(b), whose artificial dangling bonds were saturated with hydrogen, were extracted to represent H–S(100)-2×1 and H–Si(111)-1×1 surfaces, respectively. Also in these models, collisions between terminal hydrogen atoms were carefully avoided. Because the semiempirical AM1 method is able to reproduce the stability order of oxygen configurations as discussed below, and because the models are too large to be treated with *ab initio* methods, AM1 was adopted for all of the calculations with large models. From 1 to 5 oxygen atoms were inserted into Si–Si bonds constituting the upper three layers as indicated by arrows in Fig. 4, and their respective energies were calculated. As it was revealed from the study with small models that Si–O prefers to aggregate rather than to be isolated, oxygen insertion at a distant site from other oxides was excluded from consideration unless of particular interest. Furthermore, configurations with oxygen bonded to Si atoms at boundary, which are terminated by artificial hydrogen, were also omitted because the relaxation effect would not be estimated properly in such cases.

In *ab initio* molecular orbital calculations, valence double zeta basis functions with effective core potential (LANL2DZ) were employed, and for the structures optimized at the restricted Hartree–Fock (RHF) level without any constraints on the geometrical variables including those of terminal hydrogen, energies were evaluated at MP2 level. In semiempirical molecular orbital calculations (AM1), structures were also fully relaxed with no constraints and the final energies were collected. GAUSSIAN94[27] and MOPAC93[28] were used for *ab initio* and semiempirical calculations, respectively.

III. RESULTS

The most stable configurations with 1–5 oxygen atoms inserted into the small models of H–Si(100)-2×1 and H–Si(111)-1×1 surfaces are shown in Figs. 5(a) and 5(b), respectively. Bonding energies (ΔE) calculated by *ab initio* method are given under each structure. Since the most stable oxygen configuration with five oxygen atoms is not comprised of that at the previous oxidation stage on H–Si(111)-1×1, the energy does not correspond to the oxygen bonding energy but includes also the oxygen migration energy, hence it is given in parentheses. The second most stable configuration, having four oxygen atoms at the same positions as those of the most stable configuration with four oxygen atoms, is also shown and will be used in the following discussion. The structures and the corresponding bonding energies of oxidized pentasilane are given in Fig. 5(c). Also in Fig. 5, some Si atoms are supplied with Mulliken atomic charges. Atomic charges on Si are seen to increase discretely as the oxygen coordination number increases from 0 to 4, which is consistent with the previous density functional theory (DFT) calculations.[20] Since core electrons are approximated by ef-

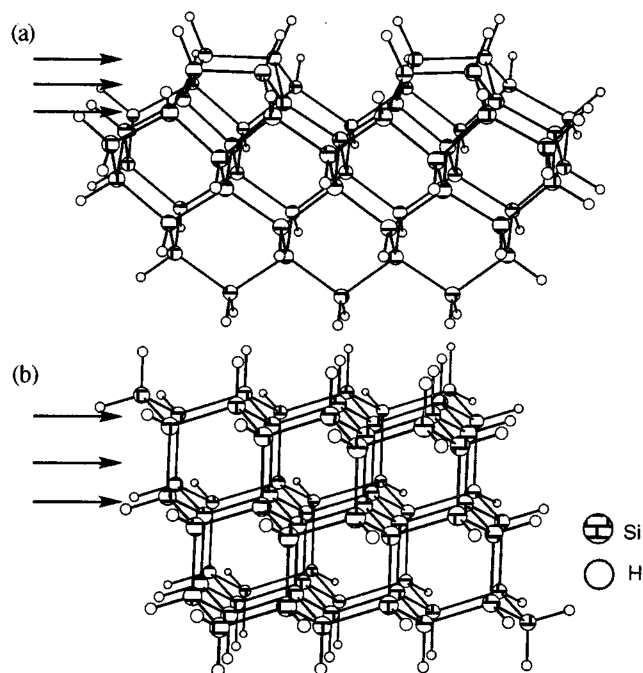

FIG. 4. Large models for (a) H–Si(100)-2×1 and (b) H–Si(111)-1×1 surfaces. Layers indicated by arrows are subjected to oxidation.

Downloaded 22 Feb 2010 to 130.34.135.21. Redistribution subject to AIP license or copyright; see http://jcp.aip.org/jcp/copyright.jsp

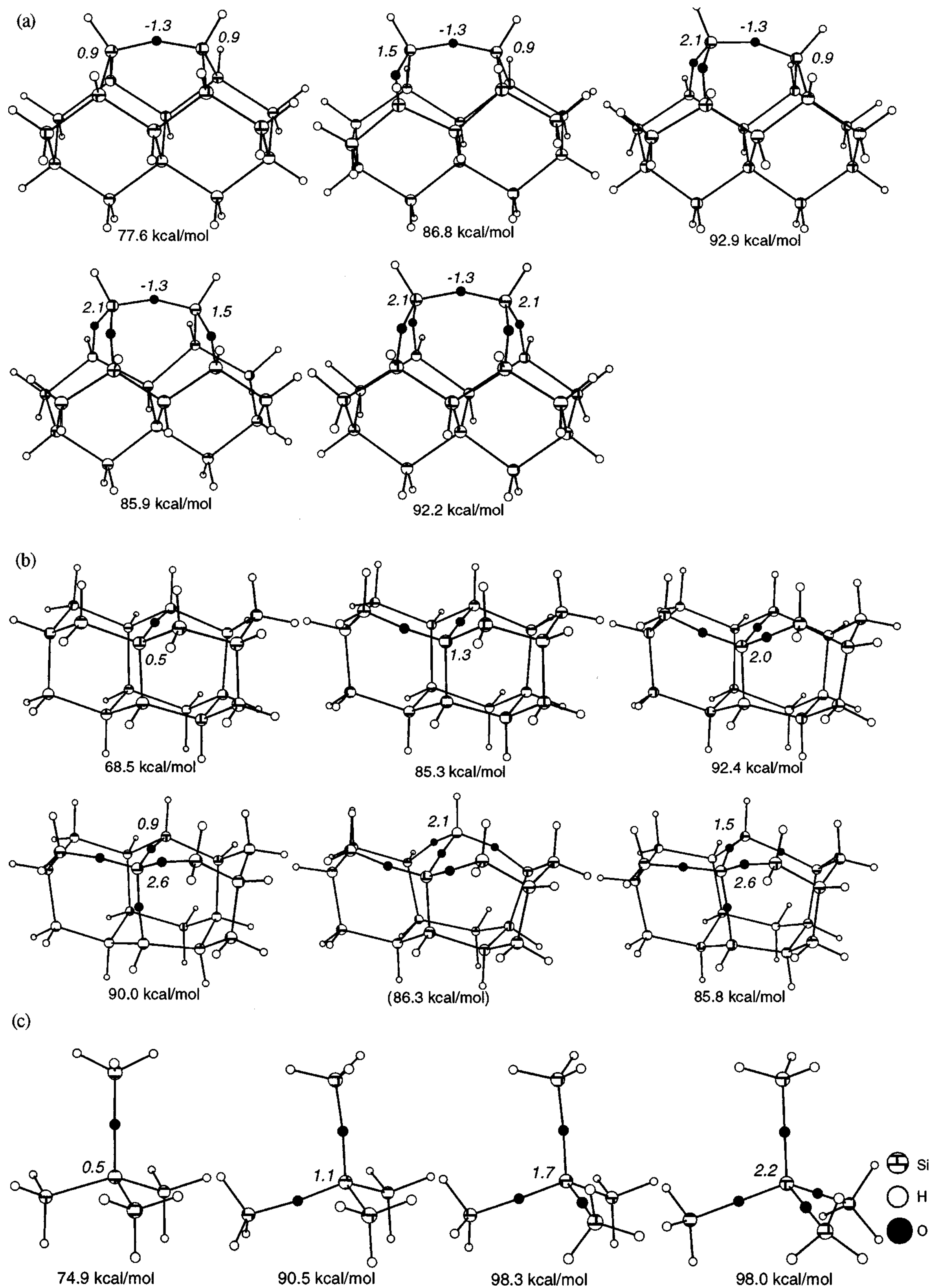

FIG. 5. The most stable oxygen configurations when 1–5 oxygen atoms are inserted into the small models of (a) H–Si(100)-2×1 and (b) H–Si(111)-1 ×1 surfaces and (c) the oxidized pentasilane molecule. Oxygen bonding energies are given under each structure. Mulliken atomic charges on some atoms are given by *italic* numbers. The second most stable configuration with five oxygen atoms on H–Si(111)-1×1 is also shown.

Downloaded 22 Feb 2010 to 130.34.135.21. Redistribution subject to AIP license or copyright; see http://jcp.aip.org/jcp/copyright.jsp

fective core potential in our calculations, core level shifts which can be observed directly by XPS are not obtainable here. However, it is known that the core level is closely related to the charge on that atom, hence five distinct Si $2p$ peaks associated with the oxygen coordination number ranging from zero to four are expected from our results, and are indeed found in XPS spectra.

The relative energies of all configurations with 1 or 2 oxygen atoms inserted into the small model of H–Si(100)-2×1 were calculated as the differences from the most stable configuration with respective number of oxygen by the semiempirical AM1 method and the results were plotted against those obtained by *ab initio* calculations (Fig. 6). Because a semiempirical method requires much less computational resources than an *ab initio* method does, the former is particularly useful to deal with large models and/or a large number of cases. However, as the name indicates, empirical parameters are used in semiempirical methods and it should therefore be tested if the target properties can be estimated with satisfying accuracy. Agreement between the two methods in Fig. 6 is excellent, and AM1 is conclusively reliable to estimate the stability order of oxygen configurations appearing in the Si oxidation process.

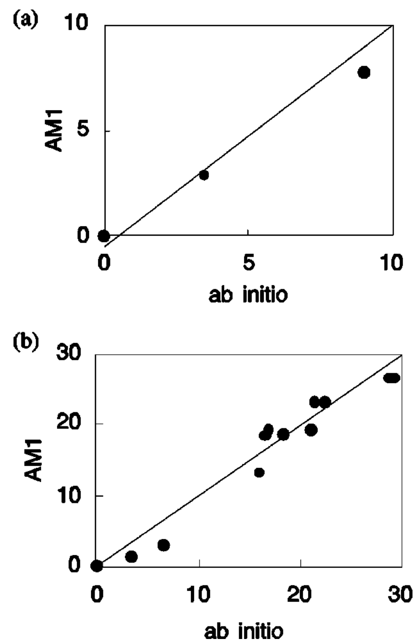

FIG. 6. Comparison of the relative energies (kcal/mol) calculated by *ab initio* and by AM1 of all configurations with 1 (a) and 2 (b) oxygen atoms inserted into the small model of H–Si(100)-2×1.

At each oxidation stage with 1–5 inserted oxygen atoms, the stability of various oxygen configurations was compared using large models. Three noteworthy oxygen configurations at each oxidation stage of H–Si(100)-2×1 are illustrated in Figs. 7(a)–7(e), respectively. Energies given under the structures are the differences from the most stable configuration at each oxidation stage. The most favorable position for the first oxygen on H–Si(100)-2×1 is the dimer site [Fig. 7(a)]. This result supports the report of Hattori *et al.*[6] Second oxygen also favors the best to be inserted into another dimer site [Fig. 7(b)]. However, while the insertion of oxygen into the second layer was less favorable than that into the first layer (dimer site) by 14.0 kcal/mol when no Si atoms are bonded to oxygen [Fig. 7(a)], the configuration obtained by the insertion under Si which is bonded to oxygen and that obtained by the oxidation of another dimer site are of nearly equal stability [Fig. 7(b)]. This small energy difference suggests that from the very beginning of oxidation, the first two layers will be oxidized unselectively at room temperature or higher. The most stable configuration with three inserted oxygen atoms was also obtained when three of them were placed at dimer sites [Fig. 7(c)]. When oxygen is inserted into the second layer so that it will be connected to the existing oxygen via Si, like in the case of two oxygen atoms mentioned above, the energetic disadvantage behind the most stable configuration was small. When four oxygen atoms are inserted, oxidation of four separated dimer sites no longer gives rise to the most stable configuration, but oxygen prefers to form an island of oxide by entering two neighboring dimer sites and two second layer sites which connect the dimers [Fig. 7(d)]. The insertion into the third layer was by far less favorable than that into the first or second layers at this oxidation stage (26.1 kcal/mol higher in heat of formation than the most stable configuration). The most stable configuration with five inserted oxygen atoms was comprised of the most stable one at the previous oxidation stage with the fifth oxygen at another dimer site [Fig. 7(e)]. However, the stability of the configuration obtained by the insertion into the third layer was nearly the same as that of the most stable configuration [Fig. 7(e)], hence one may expect that the inward growth of oxide and the nucleation of the oxide occurring at a distant dimer site compete with each other.

At each oxidation stage with 1–5 inserted oxygen atoms into the H–Si(111)-1×1 large model, three noteworthy oxygen configurations are illustrated in Figs. 8(a)–8(e), respectively. On this surface also, the top layer is most easily attacked by the first oxygen [Fig. 8(a)]. In the case of H–Si(111)-1×1, there are two possible configurations for two oxygen atoms to be inserted into the first layer, i.e., two oxygen atoms are bonded to the surface Si, which is terminated by H (not shown), or to the subsurface Si [Fig. 8(b)]. The latter was found to be the most favorable configuration at this oxidation stage, and the former was 8.3 kcal/mol less stable than the latter and was even less stable than the configuration with the second oxygen inserted under (subsurface) Si which is bonded to the first oxygen [Fig. 8(b)]. At the oxidation stage with three inserted oxygen atoms, the configuration obtained by the insertion of a third oxygen into the second layer was the most stable, and the one with three oxygen atoms inserted into the first layer was less favorable than that [Fig. 8(c)]. Third oxygen's preference for the second layer can be explained as follows. The density of Si–Si bonds in the plane parallel to the Si(111) surface is not even along the depth, and high in the first layer. Therefore a large strain energy is expected if three Si–Si bonds sharing one Si atom in the first layer are elongated by oxygen insertions, which forced the third oxygen to enter the inner site. In the most stable configuration with four inserted oxygen atoms, subsurface Si is coordinated by four oxygen atoms [Fig. 8(d)]. The configuration obtained by inserting all four oxy-

Downloaded 22 Feb 2010 to 130.34.135.21. Redistribution subject to AIP license or copyright; see http://jcp.aip.org/jcp/copyright.jsp

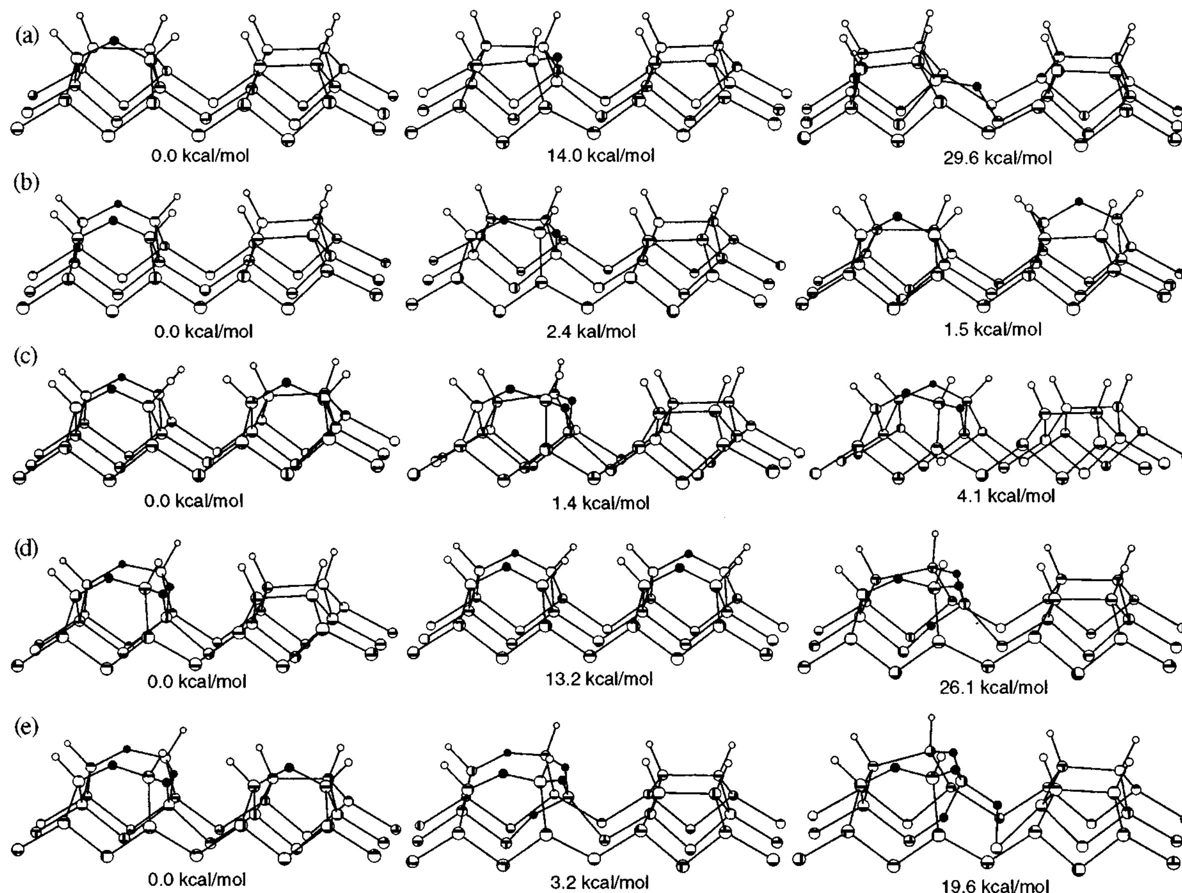

FIG. 7. Structures and their relative energies of three representative oxygen configurations at each oxidation stage of the H–Si(100)-2×1 surface: (a)–(e) correspond to the oxidation with 1–5 oxygen atoms, respectively.

gen atoms into the first layer was 10.7 kcal/mol less stable than the second most stable structure having one second layer oxygen (32.5 kcal/mol higher in heat of formation than the most stable configuration). Thus one may conclude that the second layer must be oxidized before the oxidation of the first layer is completed. The most stable configuration with five inserted oxygen atoms was obtained when the fifth oxygen was bonded to the surface Si which is already coordinated by oxygen in the most stable structure at the previous oxidation level [Fig. 8(e)]. The stability of the configurations arising from the insertion of the fifth oxygen between Si atoms which are not coordinated by oxygen in the first layer or into the third layer was inferior by 8.0 and 12.4 kcal/mol to that of the most stable one, respectively. Therefore, once a Si coordinated by four oxygen atoms is formed, oxide island will grow from this site along the lateral direction.

IV. DISCUSSION

Oxygen bonding energies (ΔE) calculated by *ab initio* method using small models are analyzed to investigate the chemistry of Si–O bonds. In Figs. 5(a)–5(c), the insertion of the first oxygen forms bonds with two Si atoms which are not coordinated by oxygen. In Fig. 5(a), one of the Si atoms bonded when the second or the fourth oxygen is inserted is coordinated by one oxygen atom, while that bonded when the third or the fifth one is inserted is coordinated by two oxygen atoms. In Fig. 5(b), one of the Si atoms bonded when the second, the third, or the fourth oxygen is inserted is coordinated by 1–3 oxygen atoms, respectively. Fifth oxygen insertion forms bonds with Si atoms coordinated by one and no oxygen atoms. From the results shown in Figs. 5(a)–5(c), the following relationship can be deduced regardless of the structure: $\Delta E_0 < \Delta E_1 < \Delta E_2 \sim \Delta E_3$, where ΔE_n is the oxygen bonding energy to a Si atom coordinated by n oxygen atoms. Therefore, as a Si forms more bonds with oxygen, it increases the affinity to another oxygen up to the third. This result is consistent with the bonding probabilities of oxygen to Si atoms in different situations, which were determined by fitting themselves to reproduce the experimentally observed oxide compositions.[6] Conclusively, since oxygen prefers Si atoms which are already bonded to oxygen, it tends to aggregate rather than to be distributed uniformly. Furthermore, the above relationship also holds in the case of (c), where four SiH_3 are not constrained in the lattice but are free from the structural strain. This tendency regarding the oxygen bonding energy of Si therefore derives from the nature of the Si–O bond itself rather than the structural relaxation effects.

In order to rationalize why Si increases the affinity to oxygen as it is coordinated by more oxygen atoms, Mulliken bonding population (BP) analyses were performed on pentasilane at each oxidation stage (Table I). The more oxygen atoms the central Si atom is bonded to, the stronger the covalency between the remaining Si–Si bonds becomes, which may contribute to the stability of the highly oxidized state as

Downloaded 22 Feb 2010 to 130.34.135.21. Redistribution subject to AIP license or copyright; see http://jcp.aip.org/jcp/copyright.jsp

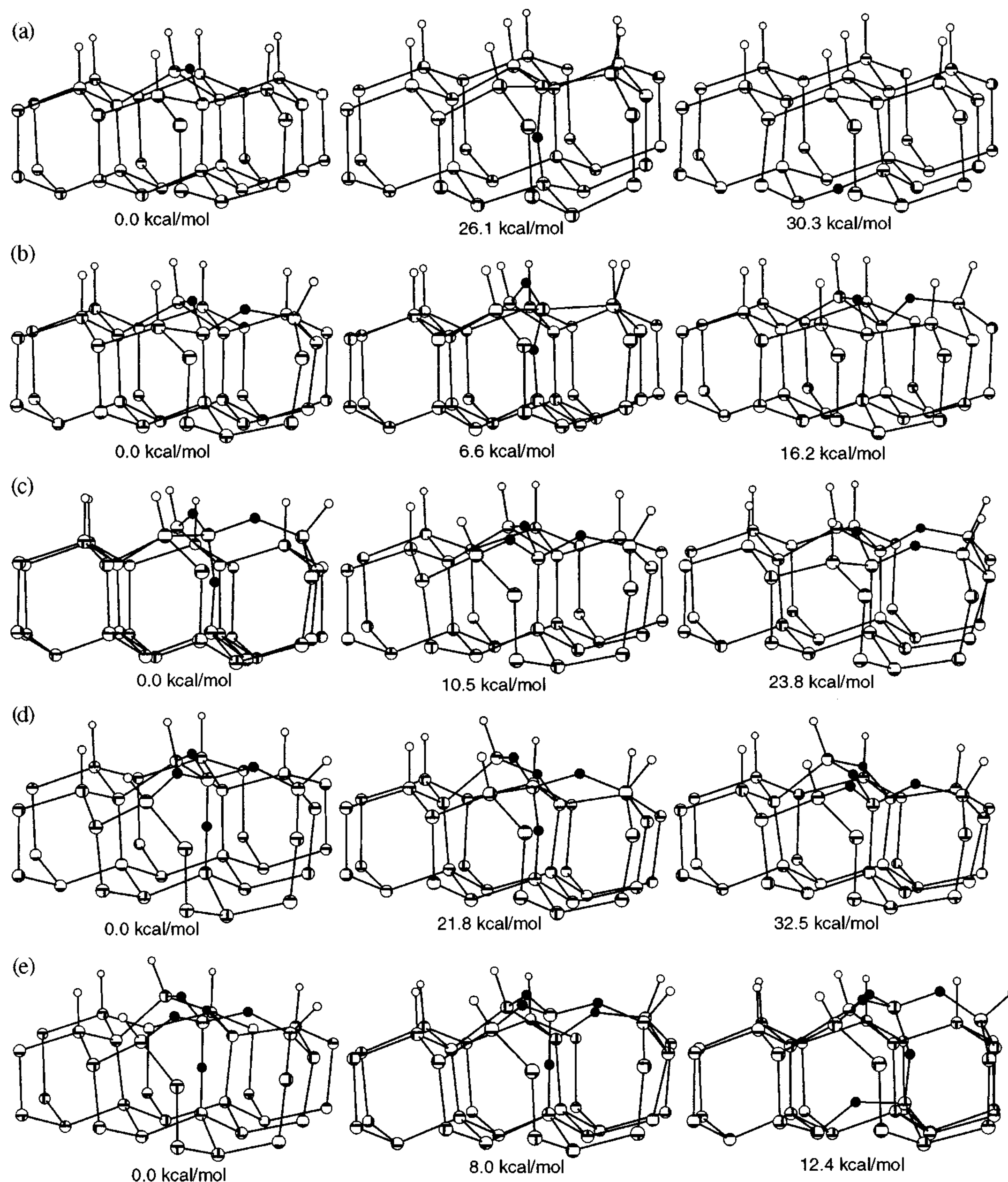

FIG. 8. Same as Fig. 7 but of the H–Si(111)-1×1 surface.

long as at least one Si–Si bond remains. The BP between the Si–O bond is small except for the one in the highest oxidation state, which indicates that the Si–O bond is not covalent but ionic. Since the atomic charge on oxygen is almost constant while that on Si increases as the oxygen coordination number increases, the Si–O ionic bond is also strengthened as Si is more oxidized.

This behavior of Si–O bonds is now examined with the results obtained with large models. As the oxidation of H–Si(111)-1×1 proceeds from one to four oxygen atoms, the oxygen coordination number of the subsurface Si in the most stable configuration increases from 1 to 4, which results in the creation of a small oxide island. On both H–Si(100)-2×1 and H–Si(111)-1×1, while it is energetically undesirable to insert an oxygen atom into the second layer when (sub)surface Si is not bonded to oxygen at all, the oxidation at the same position becomes easier once this Si is coordinated by oxygen. It can be interpreted that Si increased the affinity toward oxygen to allow the insertion of oxygen into the second layer. The most stable configuration found when three oxygen atoms are inserted into the H–Si(100)-2×1

TABLE I. Mulliken bonding population between the central Si atom and the terminal Si atom (Si–Si)/the inserted oxygen atom (Si–O) (electrons).

	Si–Si	Si–O
$Si(SiH_3)_4$	0.27	⋯
$Si(OSiH_3)(SiH_3)_3$	0.30	0.03
$Si(OSiH_3)_2(SiH_3)_2$	0.33	0.08
$Si(OSiH_3)_3(SiH_3)$	0.42	0.16
$Si(OSiH_3)_4$	⋯	0.28

Downloaded 22 Feb 2010 to 130.34.135.21. Redistribution subject to AIP license or copyright; see http://jcp.aip.org/jcp/copyright.jsp

small model was excluded from consideration in the studies with the large model because it requires the oxidation of boundary Si which is terminated artificially by hydrogen. This configuration, however, possesses a Si atom coordinated by three oxygen atoms and may be more stable than those examined here with the large model. When a fifth oxygen is inserted into the third layer of the H–Si(100)-2×1 large model [Fig. 7(e)], a bond with a Si atom coordinated by two oxygen atoms is created. According to the calculations with small models, oxygen bonding energy to a Si atom coordinated by two oxygen atoms (ΔE_2) is much higher than that to a Si atom with no oxygen neighbors (ΔE_0). Therefore the insertion into the third layer is expected to be preferred to that into the dimer site which is not bonded to oxygen. However, it is not the case probably because of the structural strain. Oxidation can hardly progress to the deeper site while the crystal structure of silicon is maintained. When five oxygen atoms are inserted into H–Si(100)-2×1, the oxygen configuration possessing a Si atom coordinated by four oxygen atoms was 19.6 kcal/mol less stable than the most favorable one [Fig. 7(e)]. As a conclusion, the structural relaxation is as important as the electronic effect on the stability of oxides.

The oxidation processes on H–Si(100)-2×1 and H–Si(111)-1×1 are now compared. The first oxygen commonly prefers to be inserted into the first layer, which is also true for the second oxygen. Also on both surfaces, the insertion into the second layer is prohibitively undesirable when no oxygen atoms are bonded to Si, but becomes easy once the (sub)surface Si is coordinated by oxygen. On the other hand, dimer sites on the H–Si(100)-2×1 surface are not connected directly with each other, hence the chances for the oxidation of two neighboring dimers and of two separated dimers are indistinguishable. On H–Si(111)-1×1, by contrast, surface and subsurface Si atoms are connected to form a network, and the second oxygen can find the position in the first layer to be connected with the existing oxygen through a Si atom. The oxidation of the adjacent sites is thus much preferred to that of the separated sites in the first layer. Therefore, it is expected that because every dimer site has an equal probability for oxidation on the H–Si(100)-2×1 surface, the nuclei of oxides will be highly dispersed and the oxidation will proceed uniformly. On the contrary, once a Si atom is bonded to oxygen, oxide is anticipated to grow from there on the H–Si(111)-1×1 surface. When three oxygen atoms are inserted, the configuration possessing a Si atom coordinated by three oxygen atoms was excluded from the consideration of H–Si(100)-2×1 due to the restriction of the model. Therefore the comparison between the two surfaces may be unfair because the most stable oxygen configuration on H–Si(100)-2×1 could have been discarded. Nevertheless, on H–Si(100)-2×1, the difference between the formation energy of three unconnected dimer oxides and that of the oxide island where three oxygen atoms are connected directly via two Si atoms coordinated by two oxygen atoms is small. On H–Si(111)-1×1, contrastingly, oxidation of the separated sites is 13.3 kcal/mol less favorable than that of the adjacent sites in the first layer which yields a Si atom coordinated by three oxygen, and is 23.8 kcal/mol less favorable than the formation of the most stable configuration which has one oxygen atom in the second layer. The growth of the oxide island should thus precede over the nucleation of oxide at a distant site on this surface. On H–Si(111)-1×1, formation of a Si atom coordinated by four oxygen atoms can be accomplished after the insertion of four oxygen atoms, while one has to wait until the oxidation proceeds much deeper on H–Si(100)-2×1 because oxygen must reach the third layer. There is no preference as the insertion point for the fifth oxygen between an isolated dimer site in the first layer and the oxide neighbor site in the third layer on H–Si(100)-2×1. Therefore, the vertical growth of the oxide island and the nucleation of oxide at a distant site occur with similar probabilities. On H–Si(111)-1×1, the fifth oxygen favors to be connected with the first layer oxygen via a surface Si rather than being inserted at the isolated first layer site or into the third layer. Thus the growth of the oxide island on the surface in the lateral direction will be dominant. These results are consistent with those obtained by the simulations using oxidation probabilities determined experimentally,[6] i.e., once an oxygen is inserted at a certain site, oxide grows in the lateral direction from there on H–Si(111)-1×1, while oxygen atoms are more uniformly distributed on H–Si(100)-2×1.

Some experimental findings in the oxidation of H–Si(111)-1×1 can be explained more reasonably from our results. Because Si atoms are connected with each other to form a network on this surface, the strain caused by the oxygen insertion is expectedly large. In polarized IR adsorption spectra of Si–H stretching, Si–H bonds inclined from the surface normal were detected.[6] Although it was explained in this report that the surface was roughened due to the oxygen insertion into the second layer, our results revealed that the Si–H bond is inclined even by the insertion into the first layer. The structural relaxation observed at an early stage of oxidation on this surface as opposed to H–Si(100)-2×1[12] can also be explained from the higher strain. Furthermore, if oxidation proceeds layer by layer, Si^{1+} and Si^{3+} must disappear alternatively. However, XPS results contradicted this expectation, and the existence of monoatomic steps was proposed.[3] From our results with three inserted oxygen atoms, it was revealed that the third oxygen prefers to enter the inner site so as to escape from a large strain, which would be produced if three oxygen atoms are inserted into the same plane. Since this structure gives rise not only to Si^{3+} but also Si^{1+}, the latter is expected to be always more than the former, which agrees with the experimental results.[3] Therefore, during the oxidation more microscopic disorder rather than monoatomic steps exists at the SiO_2/Si interface.

V. CONCLUSION

Initial oxidation processes of hydrogen terminated Si(100)-2×1 and Si(111)-1×1 surfaces were investigated by molecular orbital calculations using two types of cluster models, namely small and large models. *Ab initio* calculations using small models revealed that as a Si atom is bonded to more oxygen atoms, it increases the affinity toward another oxygen but up to the third. The reason for this is the increased covalency between the remaining Si–Si bond and

Downloaded 22 Feb 2010 to 130.34.135.21. Redistribution subject to AIP license or copyright; see http://jcp.aip.org/jcp/copyright.jsp

the strengthened ionic interaction between Si and O, which was manifested by the bonding population analyses. Semiempirical AM1 method was also proven to be reliable in the prediction of stability order of oxygen configurations from the comparison with *ab initio* results. Using the AM1 method, insertions of up to five oxygen atoms into Si–Si bonds of large models were examined. The structural relaxation was found to be as important as the electronic effect on the stability of oxides. It was also revealed that on the H–Si(100)-2$\times$1 surface, the growth of the oxide island and the nucleation of oxide at a distant site have almost the same probabilities because the surface dimer sites are not directly bonded with each other. In contrast, the lateral growth of the oxide island is preferred to the formation of isolated oxide nuclei on H–Si(100)-1$\times$1 surface because the surface and subsurface Si atoms are connected to form a network. Also on the H–Si(100)-1$\times$1 surface, the second layer was predicted to be oxidized before the completion of the first layer's oxidation due to a large strain which would be induced if oxygen atoms are inserted only into the crowded first layer.

[1] K. Goto, T. Aoyama, T. Yamazaki, and T. Ito, IEICE SDM **92-49**, 33 (1992).
[2] G. S. Higashi, R. S. Becker, Y. J. Chabal, and A. J. Becker, Appl. Phys. Lett. **58**, 1656 (1991).
[3] K. Ohishi and T. Hattori, Jpn. J. Appl. Phys., Part 2 **33**, L675 (1994).
[4] T. Aiba, K. Yamauchi, Y. Shimizu, N. Tate, M. Katayama, and T. Hattori, Jpn. J. Appl. Phys., Part 1 **34**, 707 (1995).
[5] A. Kurokawa and S. Ichimura, Appl. Surf. Sci. **100/101**, 436 (1996).
[6] T. Hattori, T. Aiba, E. Iijima, Y. Okube, H. Nohira, N. Tate, and M. Katayama, Appl. Surf. Sci. **104/105**, 323 (1996).
[7] K. Inanaga, T. Nakahata, T. Furukawa, and K. Ono, Appl. Surf. Sci. **100/101**, 421 (1996).
[8] T. Miura, M. Niwano, D. Shoji, and N. Miyamoto, Appl. Surf. Sci. **100/101**, 454 (1996).
[9] M. Ohashi and T. Hattori, Jpn. J. Appl. Phys., Part 2 **36**, L397 (1997).
[10] K. Ohmori, H. Ikeda, H. Iwano, S. Zaima, and Y. Yasuda, Appl. Surf. Sci. **117/118**, 114 (1997).
[11] H. Ikeda, K. Hotta, S. Furuta, S. Zaima, and Y. Yasuda, Appl. Surf. Sci. **104/105**, 354 (1996).
[12] H. Ikeda, Y. Nakagawa, M. Toshima, S. Furuta, S. Zaima, and Y. Yasuda, Appl. Surf. Sci. **117/118**, 109 (1997).
[13] K. Nakamura, S. Ichimura, and H. Shimizu, Appl. Surf. Sci. **100/101**, 444 (1996).
[14] X. M. Zheng and P. V. Smith, Surf. Sci. **232**, 6 (1990).
[15] A. Markovits and C. Minot, J. Mol. Catal. A: Chemical **119**, 185 (1997).
[16] P. V. Smith and A. Wander, Surf. Sci. **219**, 77 (1989).
[17] Y. Miyamoto and A. Oshiyama, Phys. Rev. B **41**, 12680 (1990).
[18] T. Oshiro, C. K. Lutrus, D. E. Hagen, and S. H. S. Salk, Solid State Commun. **100**, 439 (1996).
[19] B. Schubert, P. Avouris, and R. Hoffmann, J. Chem. Phys. **98**, 7606 (1993).
[20] H. Kageshima and M. Tabe, Surf. Sci. **351**, 53 (1996).
[21] X. M. Zheng and P. V. Smith, Surf. Sci. **279**, 127 (1992).
[22] B. I. Craig and P. V. Smith, Surf. Sci. Lett. **226**, L55 (1990).
[23] T. Watanabe, T. Hoshino, and I. Ohdomari, Appl. Surf. Sci. **117/118**, 67 (1997).
[24] P. Nachtigall, K. D. Jordan, and K. C. Janda, J. Chem. Phys. **95**, 8652 (1991).
[25] J. E. Northrup, Phys. Rev. B **44**, 1419 (1991).
[26] H. Kageshima and K. Shiraishi, Proc. ACSI-4 (in press).
[27] GAUSSIAN 94, Revision C.3, M. J. Frisch, G. W. Trucks, H. B. Schlegel, P. M. W. Gill, B. G. Johnson, M. A. Robb, J. R. Cheeseman, T. Keith, G. A. Petersson, J. A. Montgomery, K. Raghavachari, M. A. Al-Laham, V. G. Zakrzewski, J. V. Ortiz, J. B. Foresman, J. Cioslowski, B. B. Stefanov, A. Nanayakkara, M. Challacombe, C. Y. Peng, P. Y. Ayala, W. Chen, M. W. Wong, J. L. Andres, E. S. Replogle, R. Gomperts, R. L. Martin, D. J. Fox, J. S. Binkley, D. J. Defrees, J. Baker, J. P. Stewart, M. Head-Gordon, C. Gonzalez, and J. A. Pople, Gaussian, Inc., Pittsburgh, PA, 1995.
[28] MOPAC 93, J. J. P. Stewart and Fujitsu Ltd., Tokyo, Japan.

Downloaded 22 Feb 2010 to 130.34.135.21. Redistribution subject to AIP license or copyright; see http://jcp.aip.org/jcp/copyright.jsp